Publishing House
AKAPIT

COMPUTER METHODS IN MATERIALS SCIENCE

Informatyka w Technologii Materiałów

Vol. 12, 2012, No. 3

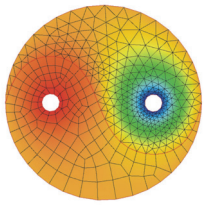

ON THE SIMULATION OF RECRYSTALLIZATION TEXTURES USING A 3D MONTE CARLO MODEL

KNUT MARTHINSEN*, EGIL FJELDBERG

Department of Materials Science and Engineering, Norwegian University of Science & Technology, N-7491 Trondheim, Norway
**Corresponding author: knut.marthinsen@material.ntnu.no*

Abstract

The texture predictions of a 3D Potts Monte Carlo (MC) model have been investigated. The model simulations are based on limited experimental input, i.e. only the initial deformation texture (i.e. a typical aluminium rolling texture) in terms of an orientation distribution function (ODF). The MC model predictions have been compared to texture simulations by a statistical recrystallization texture model due to Engler, which has been successfully applied to simulate recrystallization textures for a variety of Al alloys. In general the MC texture predictions are not satisfactory and in some cases deviate considerably from the predictions given by the Engler model. In particular, the Cube texture component, which often dominates recrystallization textures in aluminium alloys, is generally underestimated while on the other hand the retained deformation texture is too strong. The sensitivity of the texture predictions to variations in simulation conditions, related mainly to growth aspects, as well as local texture effects, is found to be limited. However, by artificially increasing the nucleation probability of Cube or by adding a small volume fraction of Cube to the nucleation texture, a significant increase of Cube may be obtained. This observation emphasise the nucleation aspect, i.e. oriented nucleation, as a key to adequately model recrystallization textures.

Key words: Recrystallization textures, Aluminium, Computer simulations, Potts Monte Carlo

1. INTRODUCTION

Microstructure control during thermo-mechanical processing of aluminium alloys is essential to optimise alloys and processes to specific applications. In this context recrystallization is a key process, where the evolution in microstructure and textures results from a complex interplay between the material's microchemistry (alloy composition and how the alloying elements are distributed between solutes, constituent particles and precipitates) and processing parameters. The recrystallization reaction has been subject to extensive investigations, both experimentally and theoretically, over several decades, but there are still important aspects of this process which are not fully understood. However, it is often difficult to identify the governing mechanisms and to single out the effect of individual parameters from experiments alone. Therefore, it is important to have adequate simulation tools for analyses and numerical experiments to explore parameter relationships which are not easily available experimentally.

Brahme (Brahme, 2005; Brahme et al.; 2006 Brahme et al., 2009) have recently proposed a procedure for reconstructing 3D experimental deformation microstructures, including texture, in terms of crystallographic grain orientations and the misorientation distribution function (MDF). Starting from such a digitally reconstructed microstructure and also experimental input about the orientation distribution (texture) and spatial distribution of recrystallization nuclei, Brahme and co-workers have also

 ISSN 1641-8581

demonstrated that the texture evolution during recrystallization (RX) of a commercial purity aluminium alloy can be well described with a 3-D Potts Monte Carlo (MC) model, which takes into account anisotropy effects in stored energy (dependent on texture), grain boundary energies and mobilities (dependent on misorientation).

In general, such detailed experimental information about the deformed microstructure is not easily available and requires thorough and tedious work to acquire. Relying on simulations alone, it is typically only the deformation texture in terms of an orientation distribution function (ODF) that is available. In the present work we have taken an experimentally determined ODF and a generic deformation structure with a random misorientation distribution as basis for 3D MC RX simulations using the MC-model of Brahme (Brahme, 2005; Brahme et al. 2009). The objective has been to investigate the characteristics of the texture predictions with this as the only (experimental) input, and in particular carry out a thorough sensitivity analysis to a variety of simulation conditions and a number of model parameters. The different simulation conditions relevant to texture, and which are possible to change in the model, include a nucleation probability table (explained in more detail below), misorientation-dependent grain boundary energy and grain boundary mobility functions, including the special energy and mobility characteristics of coincident site lattices (CSL), and in principle an orientation (texture) dependent stored energy (not used in the present work). Moreover, the spatial distribution of grains with crystallographic orientations consistent with the given texture (ODF), may be varied to give various misorientation distribution functions (MDFs).

The present MC texture predictions are partly discussed in view of the work of Brahme et al. (2009). However, for a direct comparison we have used a statistical recrystallization texture model developed by Engler (1999), a model which has been extensively validated and proven to give reliable recrystallization texture predictions for a range of aluminium alloys and processing conditions (Engler, 1999; Engler et al., 2007). This latter model approach is based on the assumption that recrystallization textures of Al alloys evolve by a preferred formation of some orientations at characteristic nucleation sites and a subsequent growth selection of distinct orientations out of this spectrum of nucleus orientations (Engler, 1996).

2. COMPUTER SIMULATION METHOD

2.1. The 3D Potts Monte Carlo model

The main simulation tool used in the present work is a 3D Potts MC model. The MC method to predict microstructure and texture has been pioneered by Rollett and co-workers and has been extensively used to predict microstructure evolution during both grain growth and recrystallization (e.g. Rollett, 1997; Rollett & Manohar, 2004). In this method a microstructure is mapped onto a 3D lattice where each lattice site is assigned a number S_i, which has a value between 1 and Q. S_i corresponds to the orientation of the grain, Q is the total number of orientations, and all neighbouring lattice sites with the same orientation are regarded as being within the same grain, while neighbouring lattice sites with another orientation are regarded as being part of another grain, and these grains are separated by a grain boundary. Each unlike pair of neighbouring orientations, S_i and S_j, contributes with a grain boundary energy of $\gamma(S_i , S_j)$ to the total system energy. In addition each site also contributes with a stored energy, $H(S_i)$, to the total system energy, where $H(S_i) = 0$ for recrystallized grains and H is constant for deformed grains. This gives total system energy, E, defined by

$$E = \frac{1}{2}\sum_{i=1}^{N}\sum_{j=1}^{N}\gamma(S_i,S_j)(1-\delta_{S_iS_j}) + \sum_{i=1}^{N}H(S_i) \qquad (1)$$

where the first sum is taken over all lattice sites, N, the second sum is taken over the nn nearest neighbours (equal to 26 in a simple cubic three dimensional lattice) of site i and $\delta_{S_iS_j}$ is the Kronecker delta.

The evolution of the microstructure is simulated by selecting a site i at random and calculating the energy change, ΔE, which is associated with changing the orientation of site i from S_i to S_i'. This reorientation is accepted with a probability p calculated from:

$$p(S_i,S_j,\Delta E) = \begin{cases} \dfrac{\gamma(S_i,S_j)}{\gamma_m}\dfrac{M(S_i,S_j)}{M_m} & \text{if } \Delta E <= 0 \\ \dfrac{\gamma(S_i,S_j)}{\gamma_m}\dfrac{M(S_i,S_j)}{M_m}e^{\frac{-\Delta E}{k_B T\gamma(S_i,S_j)}} & \text{if } \Delta E > 0 \end{cases} \qquad (2)$$

where $M(S_i, S_j)$ is the boundary mobility of grain boundaries between orientations S_i and S_j, while γ_m and M_m are the maximum grain boundary energy and mobility, respectively. k_B is Boltzmann's constant and T is the simulation temperature. If ΔE is negative or zero the change of orientation is always accepted, while if $\Delta E > 0$ a random number, r, between 0 and 1 is generated, and if r is smaller than $p(S_i, S_j, \Delta E)$ the reorientation is accepted.

The model in its present form is due to Brahme (2005) who included anisotropic grain boundary energy and anisotropic grain boundary mobility as defined in Eq. 2. The grain boundaries are divided into low angle grain boundaries, LAGB, (misorientation $\theta \leq \theta_m$) and high angle boundaries, HAGB, (misorientation $\theta > \theta_m$). In the low energy regime the energy is expressed by the Read-Shockley (RS) equation, see Eq. 3, where θ_m is the misorientation at which the boundary becomes a high angle boundary (typically $\theta_m = 15^o$).

$$\gamma = \gamma_m \frac{\theta}{\theta_m}\left(1 - \ln\left(\frac{\theta}{\theta_m}\right)\right) \qquad (3)$$

The high angle boundary is a constant equal to γ_m, except for certain "special" boundaries with particular misorientation angles, the so-called coincident site lattice (CSL) boundaries. The special boundaries (CSLs) accounted for in this model are of the $\Sigma 3$; $\Sigma 7$, $\Sigma 13b$ and $\Sigma 19b$ types which are represented as sharp minima in the Read Shockley energy function (see figure 1(a)).

Just as the grain boundary energy, the mobility anisotropy is also dependent on the grain boundary misorientation. The "Read-Shockley mobility function" is a step function, where the mobility equals 0.001 when the misorientation is below θ_m and is equal to 0.01 when it is above (in the absence of any special boundaries; Fjeldberg & Marthinsen, 2010). The special mobility boundaries considered are $\Sigma 7$, $\Sigma 19b$ and $\Sigma 37c$ with broad peaks in the mobility function, on top of a $M = 0.01$ base level, at the corresponding special misorientation angles (figure 1(b)). The most important of these is the $\Sigma 7$ boundary, corresponding to a 40^o <111> orientation relationship, with a maximum of $M = 1$ at a misorientation angle just below 40^o. The initial size and width of these maxima and minima used in the present work are identical to the ones which have been fitted to mimic the experimental texture evolution of a hot deformed commercial purity aluminium alloy (AA1050; Brahme, 2005).

Together with this, the n-fold Way algorithm, introduced by Hassold and Holm (1993) to speed up the MC simulations, is used.

A limitation of the Monte Carlo model is that the growth rate of recrystallized grains is not linearly related to the stored energy, as pointed out e.g. by Rollett and Raabe (2001). However, this problem is mainly related to the overall transformation kinetics, and is not likely to affect the texture evolution to any significant amount, which mainly relate to the relative amount and growth rate of different orientations. The excellent MC texture predictions obtained by Brahme et al. (2009), including the texture development during transformation, also indicate that this problem should not be a major obstacle to obtain good texture predictions.

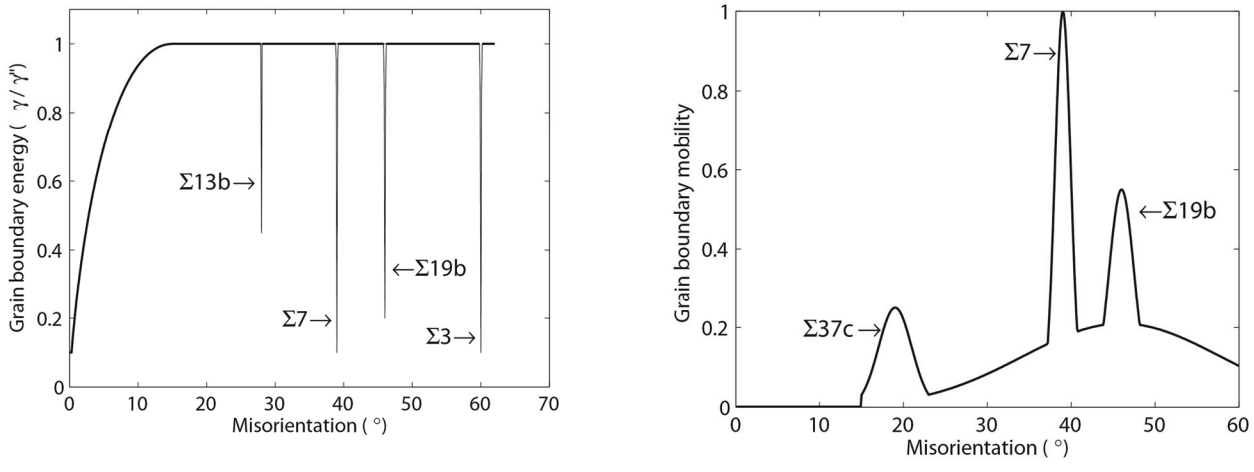

(a) **(b)**

Fig. 1. *The anisotropic grain boundary energy (a) and mobility function (b), including the "special" boundaries (CSLs), where all "special" boundaries correspond to rotations about the 111-axis($\gamma' = \gamma_m$).*

2.2. Simulation conditions

The present model simulations loosely refer to recrystallization of an aluminium alloy as a typical aluminium rolling texture is used as **input** for recrystallization simulations. It should be emphasised, however, that the present model simulations are generic and do not pretend to simulate the recrystallization behaviour of an actual aluminium alloy. The first step in the simulation setup is the generation of the initial microstructure. The present MC simulations are based on a cubical lattice of 200^3 lattice points, which is considered to be large enough to obtain statistical reliable results (Anderson et al., 1989). An initial microstructure consisting of more than 4000 grains is constructed from a modified Voronoi-tesselation type of approach to give grains with an average semi-axis ratio of 15:4:1, corresponding to the rolling direction (RD), transverse direction (TD) and normal direction (ND), respectively, of the relevant rolling experiment. These elongated grains are partly introduced to imitate a structure of elongated grains obtained experimentally with the longest semi-axis in RD and the smallest in ND. This large elongation was also used so each grain should border as many different grains as possible, and (at least) for growth orthogonal to the long axis, a recrystallized grain will be exposed to several grains of several different orientations (compromise growth; Sebald & Gottstein, 2002).

The initial deformation texture, in form of an ODF, was incorporated by discretising the ODF into about 1000 orientations, which with some additional scatter in orientations were then assigned randomly to the initial ~4000 grains, giving a so-called statistical (random) misorientation distribution function. The MDF is obtained by considering all the grain boundaries in the structure, calculating all the misorientations, and in each case take the solution with the minimum misorientation angle (from the equivalent solutions allowed by cubic symmetry), i.e. the disorientation angle, which finally are represented in form of a probability distribution $P(\theta,\Delta\theta)$, giving the fraction of boundaries with disorientation angles between θ and $\Delta\theta$ (see also Miodownik et al., 1999 for details). The statistical MDF obtained from the present input texture is shown in figure 2. Although not identical, it is seen to have clear similarities with a randomly oriented collection of grains, see e.g. Humphreys and Hatherly (2004). However, the MDF is not unambiguously defined by the texture, as the same orientations can be distributed also in a non-random manner, for instance by choosing to give neighbouring grains orientations which are close in Euler space. In the present work also starting microstructures with a spatial distribution of orientations with a maximised and minimised MDF were constructed, see figure 2, i.e. crystallographic orientations still consistent with the experimental texture were distributed in such a way as to maximise and minimise, respectively, the average disorientation between all neighbouring grains in the microstructure, to see if this change of local environment affected the final recrystallization texture. As an example, the maximum MDF, were constructed by picking at random the orientations of two neighbouring grains, and swap their orientation if the average disorientation of the microstructure is increased. The procedure is stopped when no further swaps can be found which increase the average disorientation.

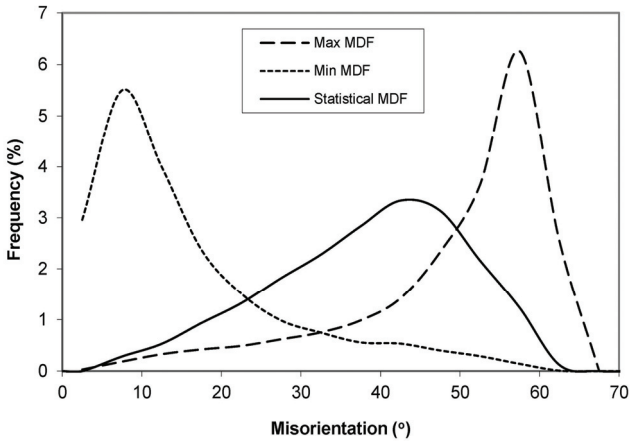

Fig. 2. *The three different MDFs used in the simulations, the original or statistical MDF and a maximised and minimised MDF, consistent with the same texture.*

The subsequent recrystallization simulations were all based on site saturated nucleation kinetics where each nucleus occupied 3 lattice sites and the initial vol% of nuclei used was 0.5. For simplicity, a constant stored energy was used, i.e. texture independent. It is well known that this is not a completely correct assumption, but because of the large difference between the grain boundary energy and the stored energy (a factor of 10), it is assumed that the relatively small differences in stored energy between the different texture components is a second order effect which only will result in minor differences in the final recrystallization texture, consistent with the findings of Brahme et al. (2009). All the MC simulations used a lattice temperature of 0.9, which is considered to be high enough to minimise the effects of anisotropy (see e.g. Brahme et al., 2009).

As a basis, the present MC simulations have been run with a standard Read-Shockley grain boundary energy, i.e. without the characteristic minima at special boundaries; cf. figure 1(a) and with a mobility of $M = 0.001$ for low misorientations ($\theta < \theta_m$) and $M = 0.01$ for large misorientations ($\theta > \theta_m$, where $\gamma_m = 15^o$ (cf. figure 1(b), without the special high mobility boundaries). For some simulations only an increased Σ7 mobility is used (cf. figure 1(a)) and more extreme variants of that, and only for a few simulations the full anisotropic grain boundary energy and mobility functions (figure 1(a) and (b)) have been used.

In line with general experience from aluminium alloys, two (three) different nucleation mechanics were considered: One corresponding to nucleation on old grain boundaries (HAGBs) (including a small fraction of Cube grains) and the second from deformation zones around large second phase particles randomly distributed in space (i.e. particle stimulated nucleation (PSN). For the latter, the orientation spectrum of nuclei is calculated according to the recrystallized texture model of Engler, i.e. a weighted 35^o<112> rotation of the deformation texture (Engler, 1999). The two nucleation orientation spectra are given in figure 3(a) and figure 3(b), respectively.

nucleation spectrum of an actual aluminium alloy. Several different grain boundary energy functions and grain boundary mobility functions were tested, and the recrystallization textures were compared with the texture as obtained from Engler's model, using the same deformation texture (ODF) and the same nucleation spectrum. Following Brahme (2005), a nucleation probability table derived for commercial purity aluminium (AA1050) was used when selecting the HAGB nuclei, see table 1. The table is binned into 5 major texture components, Cube, Brass, Copper, S and rest (e.g. Humphreys & Hatherly, 2004). The (i,j)th entry in table 1 gives the probability of finding a nucleus with an orientation close to O_i next to a deformed grain with an orientation close to O_j. It should be noted that although the figures in table 1 are consistent with experimental findings for AA1050, they also involve elements of trial and error to obtain the best possible agreement with experimental observations in terms of textures (A. Brahme, personal communication) .

Before turning to the results section, and in particular the comparisons between the texture predictions by the two models considered in this work (Engler's model and the present MC model), it may be appropriate to point out their similarities, and

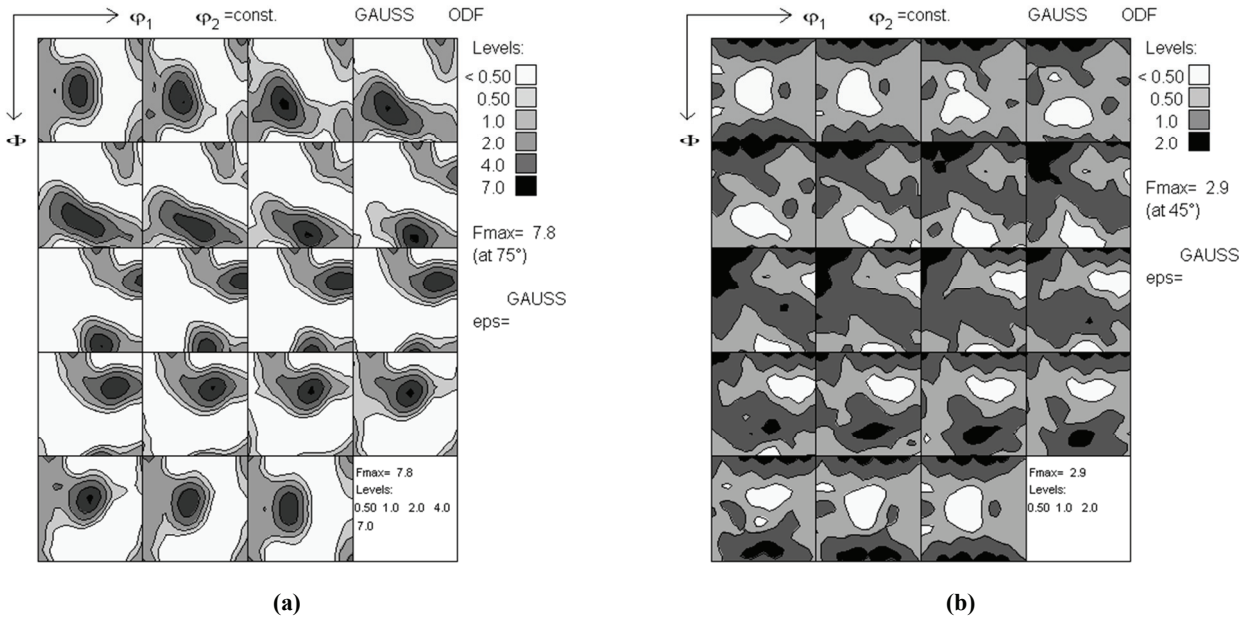

(a) **(b)**

Fig. 3. *ODFs illustrating nucleation textures for the two nucleation mechanisms. (a) The HAGB nucleation texture (inherited form the deformation texture). (b) The orientation spectrum of PSN nuclei.*

In all simulation cases, 50% of the nuclei were placed on HAGBs and the other 50% were supposed to originate from PSN and positioned randomly in the initial microstructure. It should be noted that this is just a convenient choice for the present model simulations, which does not necessarily reflect the

even more so their main differences. Although the two models are intended to simulate the same recrystallization conditions, i.e. the same initial deformation texture and nucleation conditions, the two approaches are quite different in several ways which may affect the final recrystallization texture.

Table 1. *The nucleation probability matrix used in the simulation. From Brahme (2005).*

Recryst/Def.	C	Brass	Copper	S	Rest
Cube	0.344	0.0515	0.0454	0.219	0.296
Brass	0.0727	0.355	0.0417	0.298	0.232
Copper	0.0155	0.0636	0.324	0.184	0.388
S	0.156	0.0987	0.102	0.353	0.274
Rest	0.122	0.0753	0.0548	0.203	0.522

The Engler model does not consider an explicit microstructure, and the textures are at all times represented by their ODFs only. The model does not provide any gradual texture evolution, it just gives the final transformed texture as obtained from the orientation distribution of nuclei and the growth function (Eqs. 4 and 5). Moreover a growth advantage is associated with 40° <111> boundaries only, through the growth function $f(g)^{grow}$, derived from a 40° <111> transformation of the corresponding rolling texture (Engler, 1999). The MC model on the other hand considers an explicit microstructure with grains of different size, shape and orientation, and in which, the influence of local grain boundary characteristics, such as grain boundary energies and mobilities, depending on misorientation, are accounted for. The local grain orientation relationships (spatial distribution of grain orientations) are given through an explicit MDF (not relevant for the Engler model) which has to be specified, - in absence of experimental information a statistical MDF is chosen.

A particular difference between the MC model and Engler's approach relates to the orientation spectrum of the grain boundary (GB) nucleated grains. While in the Engler model the orientation spectrum of the GB grains is derived from an artificial weakening (randomisation) of the relevant rolling texture, the actual orientations of the grain boundary nucleated grains in the MC model is the rolling texture modified through the nucleation probability matrix (cf. table 1). Further, the MC model does also, in addition to the prominent Σ7 boundaries, take into account other special boundaries (CSLs) with special energy and mobility characteristics (figure 1). These CLS boundaries have been reported in both experimental work and from atomistic simulations to have lower energies and/or higher mobilities, respectively (see Brahme et al., 2009 and references therein). Since the MC model actually follows the growth of the recrystallization grains, this model also provide the gradual evolution of the recrystallization texture, as the new grains grow to consume the initial deformed structure. Another important consequence of this is that a growing grain in general will be exposed to a number of other orientations before the recrystallization process is complete. Consequently, the growth advantage a nuclei with a 40°<111> orientation relationship to its surroundings experiences during the initial stages of growth, in general will disappear during the growth process, as this grain is exposed to other orientations, with which this special orientation relationship generally is not preserved (so-called compromise growth; Sebald & Gottstein, 2002).

3. RESULTS

The calculated recrystallization texture, with the given initial deformation texture, and by use of Engler's model with the generic nucleation conditions given above (50% GB nucleation and 50% PSN) is given in figure 4(a). In spite of the artificial (and perhaps unrealistic) nucleation conditions, the texture compares well with typical experimental recrystallization textures of aluminium alloys (Engler, 1999) (i.e. predominantly Cube with some retained deformation texture), and it is used here as a reference for the MC texture predictions presented and discussed in the following. Figure 4(b) shows the corresponding recrystallization texture as obtained from the MC simulation with Read-Shockley grain boundary energy (without the characteristic minima at special boundaries; cf. figure 1(a)) and a mobility of $M = 0.001$ for low misorientations ($\theta < \theta_m$) and $M = 0.01$ for large misorientations ($\theta > \theta_m$), where $\theta_m = 15°$. Further the original GB nucleation probability table (table 1) is used. As observed, the result compares poorly with the prediction by the Engler model, where the texture is generally much too weak, and the retained deformation texture (see figure 3(a)) seems to dominate over a very weak Cube component in the MC simulated texture.

In an attempt to improve the texture predictions by the present MC simulations and to better understand how different nucleation and growth aspects influence texture evolution, an extensive variation of various simulation conditions in the MC model has been made, including:

(i) the special energy and mobility characteristics of certain CSL boundaries,
(ii) the spatial distribution of grain orientations (different MDFs),

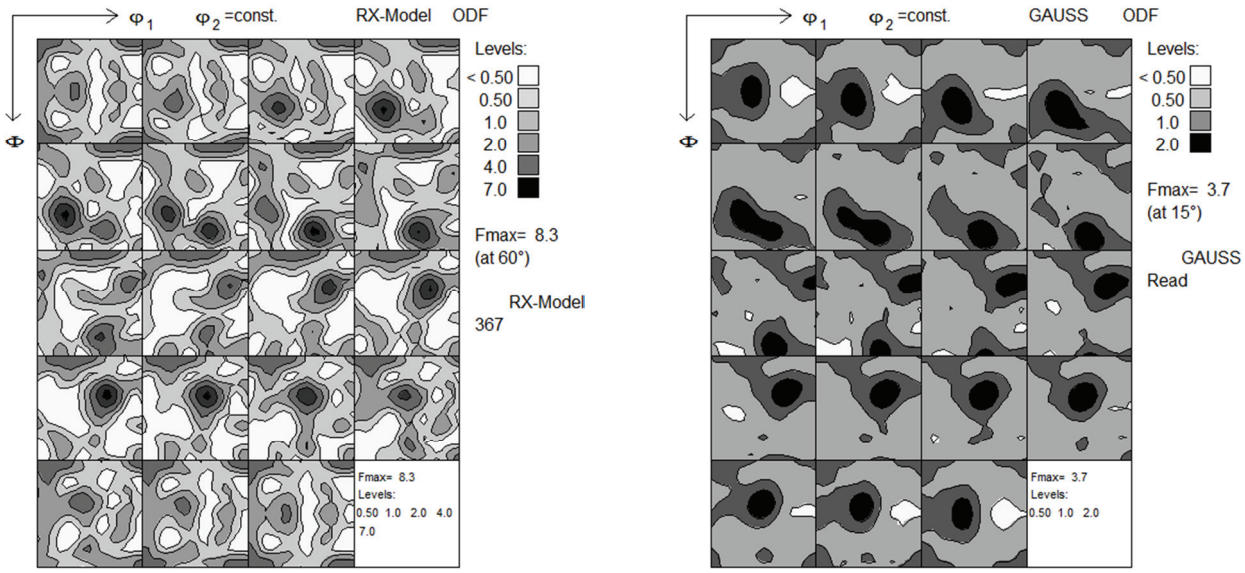

(a) **(b)**

Fig. 4. *Simulated recrystallization textures. (a) The simulated recrystallization texture from Englers model. (b) The simulated recrystallization texture with a Read-Shockley grain boundary energy and mobility M = 0.001 for low angle and 0.01 for high angle misorientations.*

Table 2. *Simulation conditions for first set of test cases.*

Σ7 mobility	Full GBE & mob. aniso	MDF	GB nucl. probability	Figure Number
-	-	Statistical	Original (from[3])	Fig. 4(b)
Original	-	Statistical	Original	Fig. 5(a)
10x orig. width	-	Statistical	Original	Fig. 5(b)
Original	X	Statistical	Original	Fig. 6 & 7
Original	-	Max	Original	Fig. 8(a)
Original	-	Min	Original	Fig. 8(a)
4x orig. width	-	Statistical	Modified	Fig. 9

(iii) the grain boundary nucleation orientation probabilities,

(iv) the amount of cube in initial deformation texture.

A large number of variants have been tested and the results below are a selection of illustrative examples. Table 2 summarises the different conditions for which the first set of simulations were done. Column 1 indicate whether an increased Σ7 boundary mobility is included, with "original" referring to figure 1(b), and an "X" in column 2 indicates that the full anisotropic full grain boundary energy (GBE) and mobility functions (figure 1) are included. The different variations are partly rationalised (see below), however, it should also be noted that some of the variations are somewhat arbitrarily chosen and included to illustrate the influence of, or sometimes lack of influence of, rather extreme parameter variations.

3.1. Effect of CLSs

The texture in figure 4(b) refers to a simulation without the special mobility characteristics of the CLS boundaries as indicated in figure 1(b). The most prominent of the "special" boundaries is the Σ7 boundary corresponding to an approximate 40^{o}<111> orientation relationship. It is well known from literature that 40^{o}<111> boundaries are fast growing boundaries in aluminium alloys (Liebmann et al., 1956; Mykura, 1980 and references therein), and they are as such supposed to play a key role in the formation of typical recrystallization textures, especially the Cube component, in these alloys. The rationale behind this is that since Cube has a Σ7 orientation relationship towards other important deformation texture components, e.g. S (Vatne et al., 1996), Cube orientated grains will then also assumedly be subjected to a growth advantage promoting the Cube texture development. This is also the basis for the growth selection in Engler's model (1999).

On this basis we have carried out simulations with a greatly enhanced mobility for the Σ7 type boundaries, to possibly single out effects of these special boundaries (figure 5). Two particular cases have been simulated, one with the mobility characteristics of Σ7, as given in figure 1(b) (denoted **orig-**

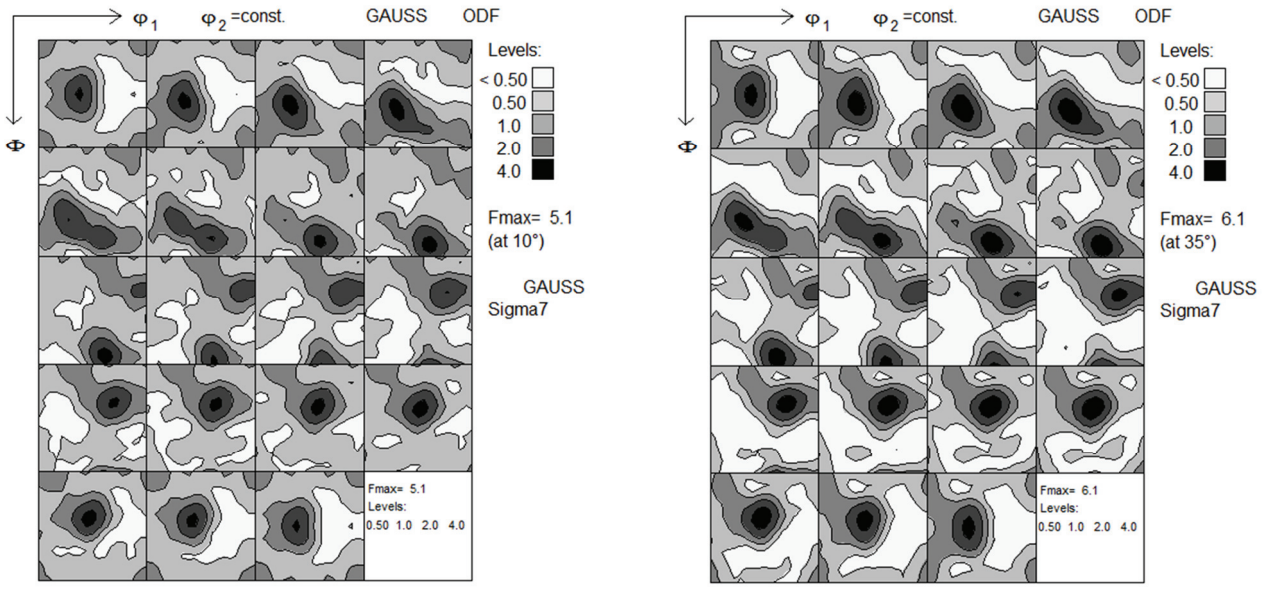

(a) **(b)**

Fig. 5. *Simulated recrystallization textures with a Σ7 peak in the mobility function. (a) MC simulated texture with the "original" narrow Σ7 mobility. (b) MC simulated texture with an extremely increased width of the mobility peak around Σ7.*

inal and taken from Brahme, 2005), and a second one with an extremely wide Σ7 mobility (with a width 10 times the "original"). Both simulations are carried out with the same "original" grain boundary energy, i.e. the Read Shockley energy function, Eq. 3. However, although a distinct influence is observed, and the resulting MC recrystallization textures (figure 5) may look closer to the reference texture (figure 4(a)), they are still somewhat too weak and in particular the strength of the Cube is much too low. It is also noticed that the differences between these two simulated cases are small, even though the simulations are run with quite different mobility functions.

Next step is simulations with the special energy and mobility characteristics of all the CSL boundaries included in figure 1(a) and figure 1(b) (indicated with an "X" in column 2 of Table 2). The resulting final recrystallization texture is presented in figure 6. Again, there are only minor differences between this result and the previous MC simulated recrystallization textures, especially those in figure 5.

To get a better insight into how the texture develops during the recrystallization reaction, the present MC model also offers the possibility of tracing the development of certain prominent texture components during the recrystallization process. This is exemplified in figure 7 which refers to the same simulation case as in figure 6. The texture components followed (in terms of name and Euler angles) are, the Cube orientation (0°; 0°; 0°), Goss (0°; 45°; 0°), Brass (35°; 45°; 0°), Copper (40°; 65°; 26°) and S (64.93°; 74.50°; 33.69°). As can be seen, there is a clear decrease in all the strong deformation texture components, especially for the S and the Brass components, while any increase in Cube is not observed, instead the Cube is quite stable at a volume fraction of 0.03, consistent with the ODF in figure 6, but different from the texture predicted by Engler's model, where the presence of Cube is quite clear.

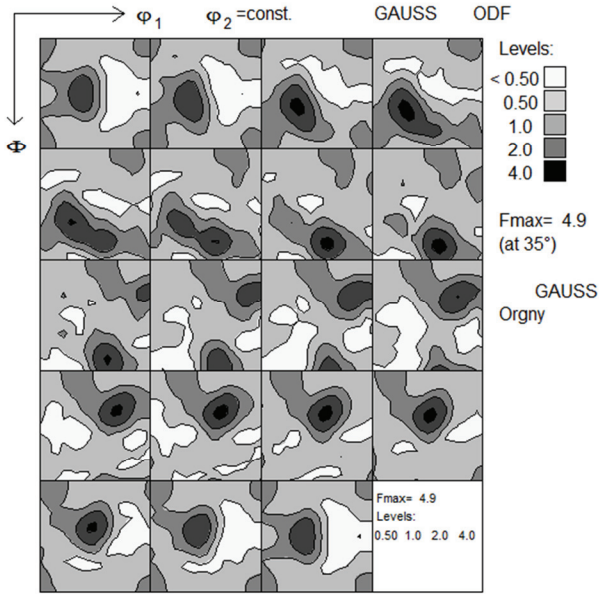

Fig. 6. *The MC simulated recrystallization texture with grain boundary energy and mobility as shown in figure 1 (a) and figure 1 (b).*

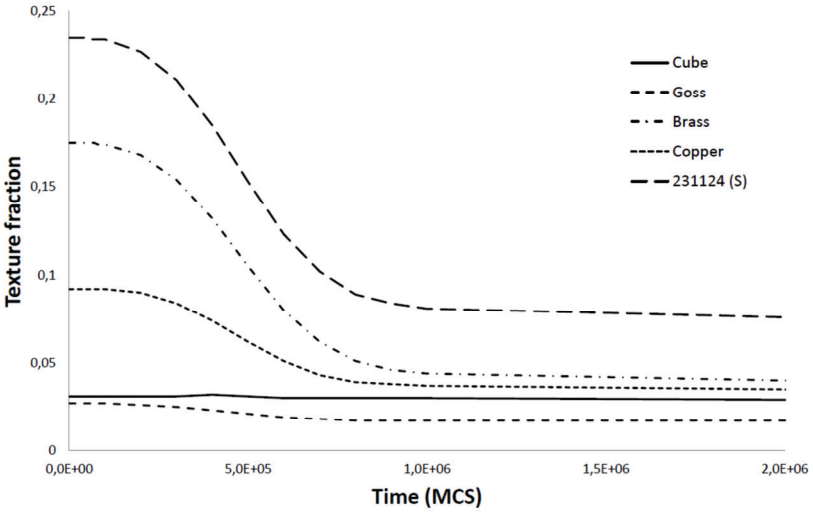

Fig. 7. The texture development until 100% recrystallized for the simulation with fully anisotropic grain boundary energy and mobility (cf. figure 1).

tions, on the other hand, in lack of this particular information are based on a statistical MDF, consistent with the initial deformation texture (input ODF). However, as pointed out above the MDF is not unambiguously given by the texture, and the same texture may correspond to a different spatial distribution of the grain orientations, i.e. local differences in grain environment. For this reason, the effect of varying the MDF has also been tested out, but also in these cases without any significant effects. This is illustrated in figure 8, referring to two rather extreme cases, i.e. a MDF where the average misorien-

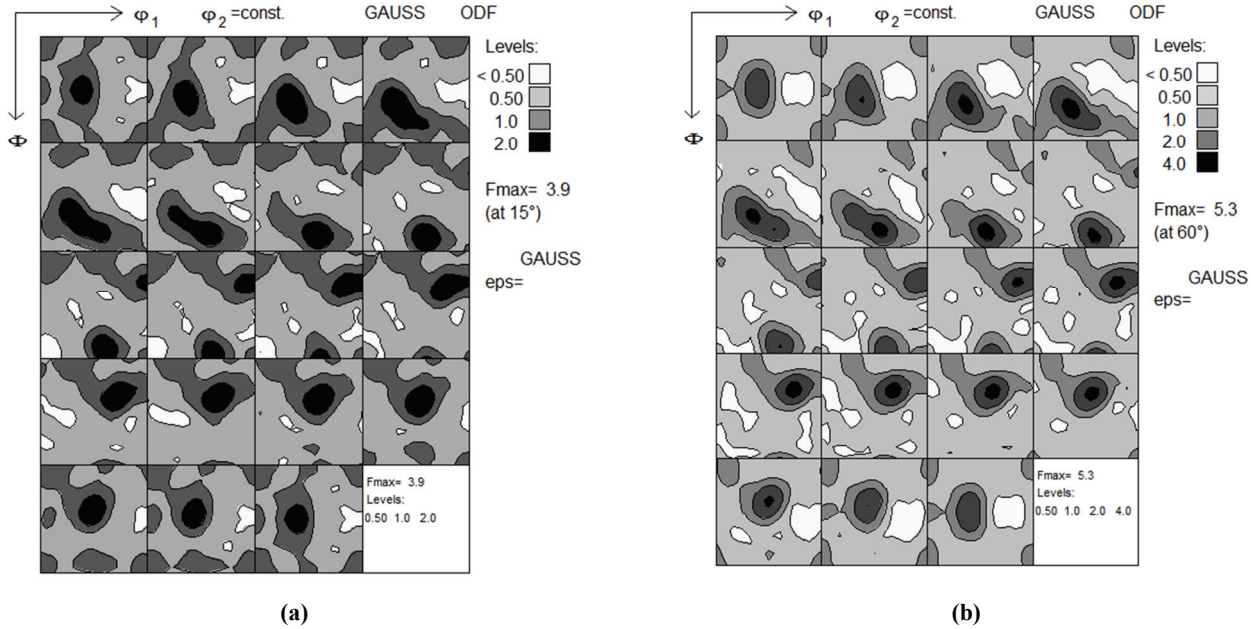

(a) **(b)**

Fig. 8. Recrystallization textures with Σ7 grain boundary energy and boundary mobility and a modified MDF. (a) MC simulated texture with "original" Σ7 and the maximised MDF seen in figure 2. (b) MC simulation texture with "original" Σ7 and the minimised MDF seen in figure 2.

Neither is this texture development consistent with Brahme's results (Brahme, 2005; Brahme et al., 2009), where the Cube texture was strongly increased from a volume fraction of around 0.07 to approximately 0.33 after 10^6 Monte Carlo Steps (MCS). On the other hand, both S, Brass and Copper also decreased in their simulations. However, compared to experiments, an even stronger decrease in S was observed.

3.2. Effect of Misorientation Distribution Function (MDF)

Brahme et al. (2009) used an experimental MDF as basis for their simulations. The present simulation was maximised and another MDF where the average misorientation was minimised, see figure 2. Both cases were run with the original Σ7 mobility as shown in figure 1(b). As for the previous simulation cases considered, no significant influence on the recrystallization textures is obtained. Only a few minor differences are observed, i.e. the maximised MDF results in a minor weakening and widening of the retained deformation texture (as compared to figure 5(a), which except for the MDF uses the same simulation conditions), while the minimised MDF on the other hand is almost identical to the ODF in figure 5(a)).

3.3. Effect of grain boundary nucleation probabilities

The results so far indicate that the cube nucleation is too small. Therefore, in order to increase the initial amount of Cube and by that also possible effects of Σ7 boundaries during growth, the nucleation probability matrix was artificially modified to promote preferential nucleation of Cube from the given deformation texture spectrum. Again a large number of variants have been tested, however, only one example is discussed below to illustrate the effect of justified, but still rather extreme changes. The actual modified nucleation matrix is given in table 3. Compared to the original nucleation probability matrix (table 1) some of the values are somewhat arbitrarily changed, however, with a main purpose, to promote cube nucleation, as compared to the rest. For example all figures in the top line are increased considerably, increasing the probability of nucleating Cube next to Cube or at any of the other components, especially Cube at a Cube/S boundary, in agreement with experimental findings (e.g. Vatne et al., 1996). The resulting recrystallization texture for this particular case is shown in figure 9. It is observed that an increased cube nucleation probability has an effect on the texture predictions. The amount of cube has increased as compared to the deformation texture components, and the resulting ODF is qualitatively closer to the reference (figure 4(a)) than for most previous simulation cases, however, the texture strength is still somewhat too weak.

Table 3. *An artificially modified nucleation probability matrix used in the simulation.*

Recryst/Def.	C	Brass	Copper	S	Rest
Cube	0.744	0.3015	0.3054	0.919	0.796
Brass	0.0727	0.155	0.0417	0.1998	0.132
Copper	0.0155	0.0636	0.124	0.184	0.288
S	0.156	0.0987	0.102	0.153	0.174
Rest	0.122	0.0753	0.0548	0.103	0.422

3.4. Manipulated experimental texture input

As commented above, one of the main differences between Brahme's simulations and the present ones seem to lie in the orientation spectrum of nuclei, where the present simulations seem to be too low in Cube. Since several of the simulations considered above have shown that a growth advantage

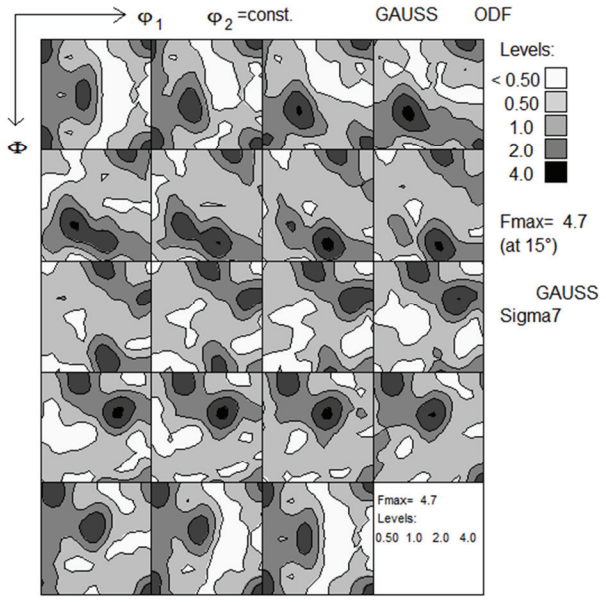

Fig. 9. *The MC simulated recrystallization texture with the nucleation table shown in Table 3 and a Σ7 mobility peak four times as wide as the one used in figure 5(a).*

is not enough to account for the amount of Cube in the final recrystallization texture, the effect of artificially adding Cube is also tested out. The Cube orientations used are randomly constructed from angles in Euler space ranging from 0^o to 5^o for both ϕ_1, Φ, ϕ_2 (perfect Cube corresponds to $\phi_1 = \Phi = \phi_2 = 0$). Next, these orientations are added to the nucleation orientation spectrum by replacing a fraction of the PSN texture orientations with these Cube orientated grains. The new PSN nucleation textures used after replacing 2.5% and 5% of the original PSN texture (figure 3(b)) is given in figure 10(a) and (b), respectively. This figure clearly shows that adding a small fraction of Cube gives a noticeable increase of Cube in the nucleation orientation spectrum (seen in the upper left corner of the first square of the ODFs in figure 10(a) and figure 10(b)). The different simulation conditions which have been run with this input are summarised in table 4 (with the meaning of the different columns as for table 2).

The resulting recrystallization texture for a simulation run with the PSN texture shown in figure 10(a) (i.e. adding 2.5% cube) and the fully anisotropic grain boundary energy and mobility as shown in figure 1(a) and figure 1(b), is shown in figure 11(a), while a simulation with the same PSN texture, but only with Σ7 anisotropy, where the mobility is widened by a factor of four compared to the original one, is shown in figure 11(b).

Table 4. *Simulation conditions for second set of test cases.*

Σ7 mobility	Full GBE & mob. aniso	MDF	Vol% extra Cube	Figure Number
Original	X	Statistical	2.5	Fig. 11(a)
4x orig. width	-	Statistical	2.5	Fig. 11(b)
Original	-	Max	2.5	Not shown
Original	-	Min	2.5	Not shown
Original	X	Statistical	5	Fig. 12(a)
Original	-	Statistical	5	Fig. 12(b) & 13

Simulations with 2.5% artificially added Cube to the PSN texture, with the "original" narrow Σ7 grain boundary energy and mobility and with the original, close to random, MDF, a maximised MDF and a minimised MDF, respectively, have also been run. However, as all these simulations gave approximately the same recrystallization textures as in figure 11, they are therefore not shown.

The results for a simulation run with the same full anisotropy as above but with 5% artificially added Cube in the PSN texture (figure 10(b)) is seen in figure 12(a), while the recrystallization texture

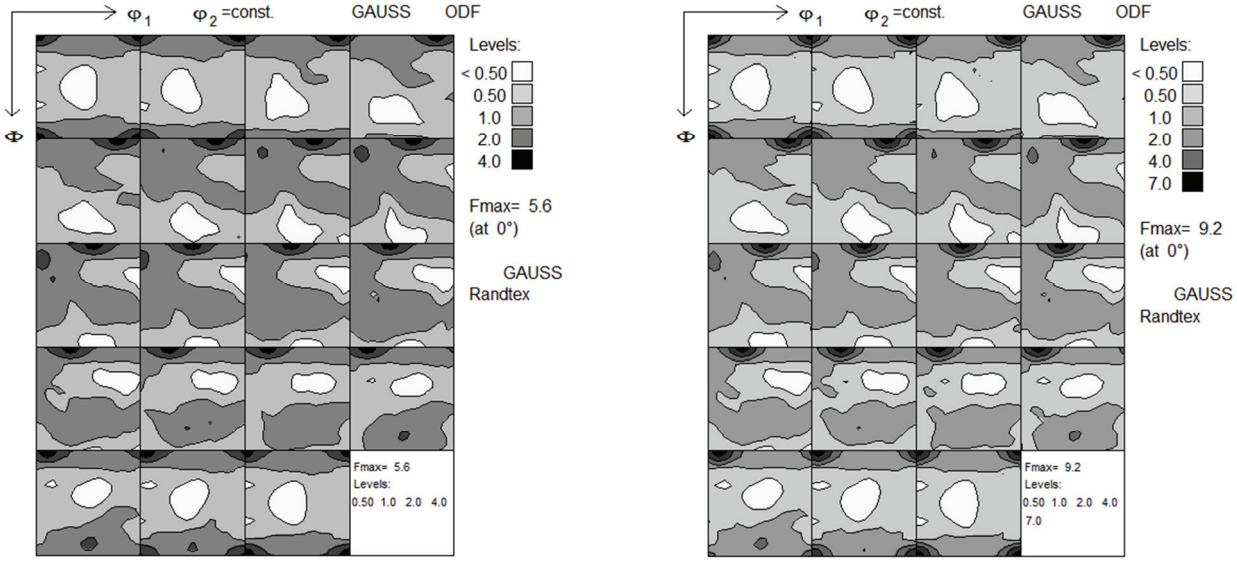

(a) **(b)**

Fig. 10. *The new PSN texture after artificially adding a small amount of Cube. (a) The new PSN texture after replacing 2.5% of the original orientations with Cube. (b) The new PSN texture after replacing 5% of the original orientations with Cube.*

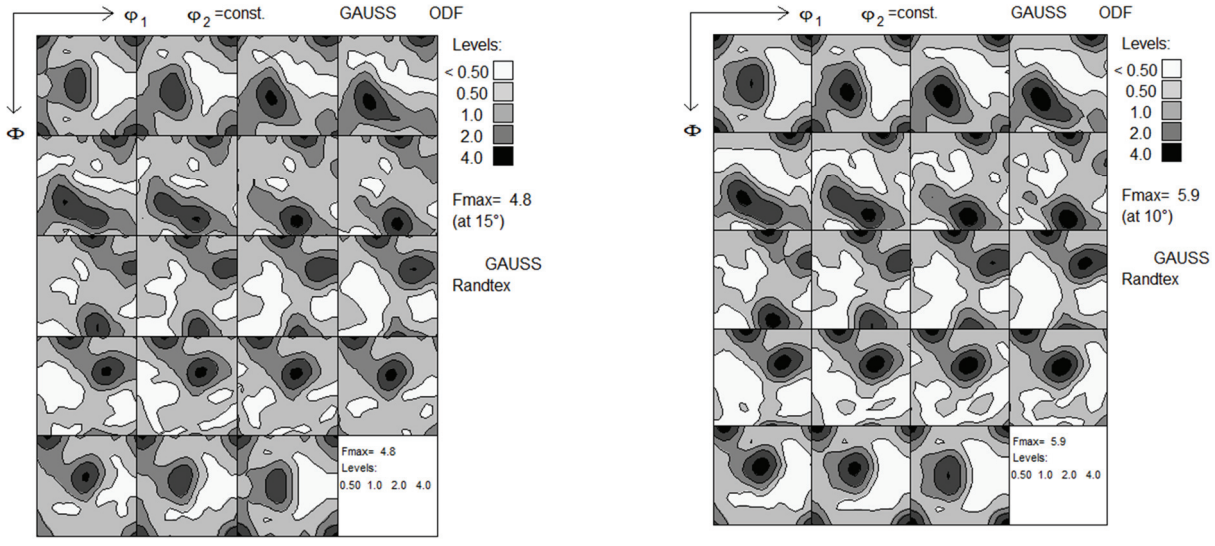

(a) **(b)**

Fig. 11. *Recrystallization textures when the PSN texture is artificially added 2.5% Cube, see figure 10(a). (a) Recrystallization texture for a simulation run with full anisotropy, see figure 1(a) and figure 1(b). (b) Recrystallization texture for a simulation run with a Σ7 grain boundary energy and mobility, where the mobility function is widened by a factor of 4.*

after a similar simulation, but only with the original Σ7 anisotropy is shown in figure 12(b). The results are quite similar to those in figure 11, i.e. the effect of the extra cube is limited.

The texture development (time evolution) has also been analysed for this latter case. The result is shown in figure 13. Comparing these curves with the ones in figure 7, an approximate doubling of the Cube texture is obtained. Except for that, only minor differences are observed.

It is evident that artificially adding extra cube to the nucleation spectrum do improve the MC texture predictions (as compared to the reference in figure 4(a)), increasing the amount of Cube also in the recrystallization textures. However, in general the textures are still too weak, and the sensitivity to other variations in the simulations conditions is limited.

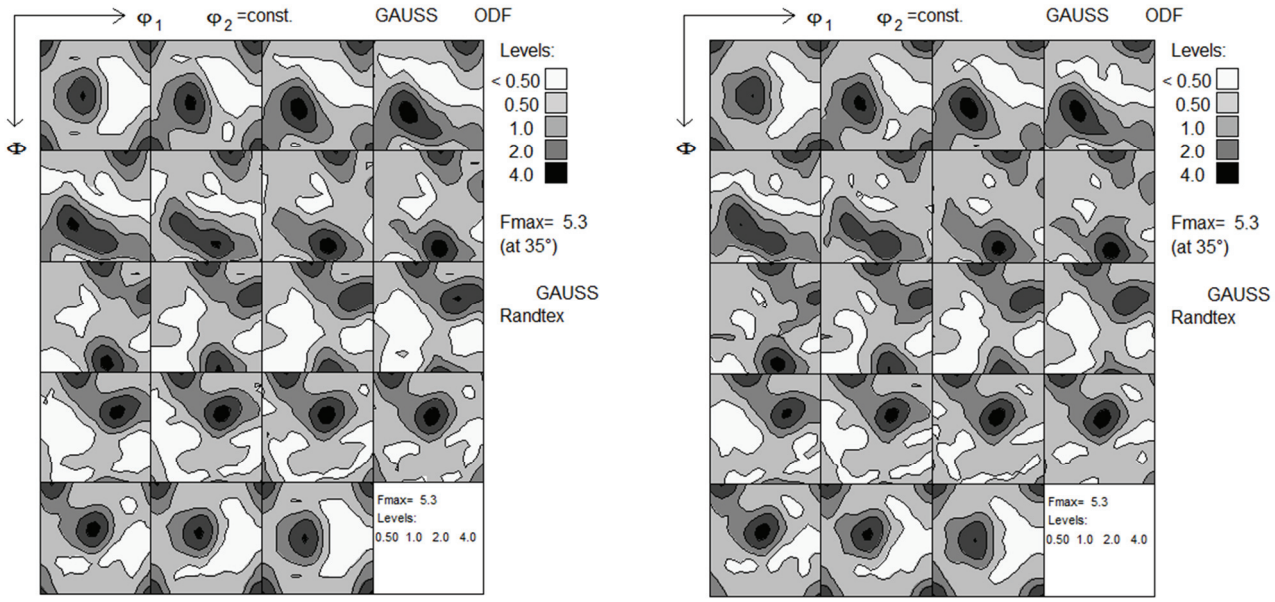

Fig. 12. *Recrystallization textures when the PSN texture is artificially added 5% Cube, see figure 10(b). (a) Recrystallization texture for a simulation run with full anisotropy, see figure 1(a) and figure 1(b). (b) Recrystallization texture for a simulation run with original Σ7 grain boundary energy and mobility.*

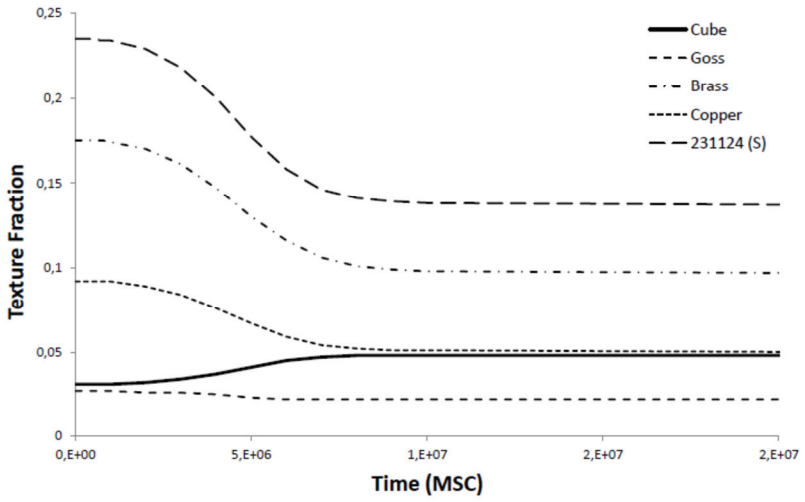

Fig. 13. *The texture development until 100% recrystallized for the simulation with 5% artificially added Cube to the PSN texture and an "original" Σ7 grain boundary energy and mobility function.*

4. DISCUSSION

The present paper has considered the texture predictions of a 3D Monte Carlo model, and the characteristics of the texture predictions using limited experimental input, i.e. only the starting texture in terms of an ODF, have been investigated. It has clearly been demonstrated that to obtain satisfactory MC texture predictions is not straightforward, both in view of typical experimental recrystallization textures for aluminium (cf. Brahme, 2005; Brahme et al., 2009) and in particular as compared to the corresponding texture predictions by the Engler model. Concerning the comparison with Brahme's results, it should be noted that Brahme's and the

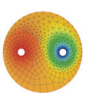

present simulations refer to different alloys (in the present case a generic one). Moreover, an even more important difference is that Brahme used an orientation spectrum of nuclei obtained from experiments, while the present simulations are based on an artificial (and perhaps unrealistic) nucleation texture, assuming 50% GB nucleation and 50% PSN. These are the same as the ones used in Engler's model, but still quite different from the ones used by Brahme. This will most probably strongly affect the texture development and final recrystallization texture. Compared to Engler's model, the deviations relate in particular to the fact that the characteristic Cube texture, which commonly dominates recrystallization textures in aluminium alloys, are generally underestimated while on the other hand the retained deformation texture is too strong. This large difference in the Cube texture development is somewhat surprising, as both models start with approximately the same deformation texture, and as pointed out above with the same orientation spectrum of nuclei (although, just with half the amount of Cube as in Brahme's deformation texture).

A special feature of the Engler model is the prominence it gives to 40^o <111> type boundaries (i.e. Σ7 boundaries) through a distinct growth selection of these boundaries. However, the same importance of Σ7 boundaries is not found in the present MC simulations. Even when the width of the Σ7 mobility function is increased by a factor of 10, no significant differences were seen in the recrystallized textures. This observation points to the fact that the growth advantage associated with Σ7 boundaries, and Cube grains, which have this orientation relationship to certain other texture components, is not enough to explain the amount of Cube in the recrystallized texture as seen in figure 4(a). This may be due to the fact that there are very few nuclei/recrystallized grains that actually involve this orientation relationship to its neighbours (see e.g. Hassold et al., 2003). Secondly, a recrystallized grain will in most cases be exposed to grains of different orientations, which generally makes it unlikely for Σ7 boundaries to be preserved all through the simulation. The reason may be that even with very elongated grains, there will be a limitation in the number of neighbouring grains, and the Σ7 aspect gives only a local growth effect, both in time and in space. For a small period of time, a grain may grow faster than the others because of a mobility advantage of the Σ7 boundaries, but exposed to other orientations the growth advantage will disappear, and this now "abnormal" grain will grow slower than the average grains until it again has an average grain size, see e.g. Humphreys and Hatherly (2004). It should be noted, though, that there are exceptions. E.g. if a Σ7 boundary grows into a textured material with a strong texture the ability to preserve a Σ7 structure is not that difficult.

In general, the present MC simulations have clearly demonstrated that the various anisotropy effects accounted for in the grain boundary characteristics, related to growth, including local variations in growth conditions through extensive variations in the MDF and in particular those related to so-called special boundaries (CSLs), including Σ7 boundaries, have a limited effect on the global texture development.

Because of the limited growth effect, the nucleation aspect is correspondingly more important, i.e. there must be mechanisms for the nucleation of Cube texture grains (oriented nucleation) which are not accounted for in the present MC simulation model. The amount of Cube in the deformation texture used in the present simulations (figure 3(a)) is much too small to account for the number of Cube nuclei necessary to reproduce the amount of Cube in the resulting recrystallization texture in figure 4(a). However, by manipulating the nucleation behaviour by promoting cube nucleation, either by artificially increasing the nucleation probability of Cube or by just by adding a small fraction of Cube to the PSN texture, the intensity of Cube is considerably increased in the recrystallization texture, as seen in figures 11-13, although still somewhat to weak, as compared to Engler's model.

What is somewhat surprising is that the present MC simulations, which intuitively seem closer to reality than the concepts of Engler's model, give poorer texture predictions. In the latter model the resulting recrystallization texture is in part determined by a mathematical transformation of the deformation texture through a 40^o <111> rotation (growth selection). Thus, in the Engler model the growth selection/advantage is associated with Σ7 boundaries alone, and moreover, a growth advantage which is preserved all through the transformation. However, in spite of this apparent deviation from what is believed to take place in real 3D polycrystalline materials, Engler's model is justified through its capability to capture the essentials of recrystallization textures in a range of aluminium alloys (e.g. Engler, 1997; Engler, 1999; Engler et al., 2007). However, an important difference, to be noted, rele-

vant for the comparison of the MC results and the texture predictions by Engler's model, is the orientation spectrum of the grain boundary nucleated grains, which is treated differently in the two models as also pointed out above. The GB nucleation probabilities used in the present work are adopted from Brahme (Brahme, 2005; Brahme et al., 2005; Brahme et al., 2009), and derived from hot rolling of an AA1050 alloy, and is strictly speaking only valid for this alloy. Using the same GB nucleation probabilities for any aluminium alloy may of course be inaccurate and cause differences. However, the present work has also shown that rather large changes in the nucleation probabilities influenced the final textures to a limited extent, which seem to indicate that this is not a major problem. To better understand the origin of the differences it would have been desirable being able to compare the texture evolution throughout the whole transformation process, from the early stages after nucleation to the fully transformed state. Unfortunately, this is not possible with the Engler model.

5. CONCLUSIONS

One of the most important findings of the present work, seems to be a demonstration of the fact that the simplified nucleation assumptions made with PSN (involving a nearly random texture) and HAGB nucleation where the nuclei mainly inherit the deformation texture orientations, combined with a growth advantage of Σ7 boundaries, are insufficient to predict typical Al recrystallization textures using the Potts MC method. Even significant (and sometimes un-physical) changes in the MDF and mainly the growth condition only resulted in minor changes in the final texture.

On the other hand, the present MC simulations do emphasise the nucleation aspect as a key to adequately explain recrystallization textures, i.e. the importance of oriented nucleation, as illustrated e.g. by the effect of artificially promoting Cube nucleation or by artificially adding Cube. Although the growth advantage of the Σ7 boundaries also has effects, it was not decisive for the present MC texture predictions. These findings are consistent with the work of Brahme et al. (2009), who also concluded that oriented nucleation is the most important factor to get the textures correct, and with respect to the Cube aspect, also with the recent experimental findings by Alvi et al. (2008), on cube texture in a hot-rolled commercial purity Al-alloy (AA1050). Therefore, an important aspect of improvements, to ensure more reliable texture predictions by the present Potts MC code, is to identify and/or rationalise additional and/or alternative nucleation mechanisms, and in particular mechanisms for the nucleation of Cube grains to be included in the nucleation assumptions used in the code. It should be noted, though, that this is not only a challenge for the Potts MC model, but relates to the understanding and modelling of recrystallization in general, for which nucleation still is a poorly understood aspect. With the current incomplete understanding of nucleation, detailed experimental input is most probably a prerequisite, as demonstrated in the work by Brahme (2005) and Brahme et al. (2009), to obtain good texture predictions by the MC approach. Brahme et al. (2009) also pointed out the importance of the stored energy and grain boundary energy, although less important than oriented nucleation and oriented growth, and more so for the gradual evolution of the texture during transformations than the actual final texture. The latter aspect was not an issue for the present work since the Engler model did not provide this information. However, it is important to have in mind for further work when this aspect also may be included.

ACKNOWLEDGMENTS

A. Brahme, C. Roberts and A.D. Rollett, Dept. of Materials Science and Engineering, Carnegie Mellon University, PA, USA are gratefully acknowledged for providing the MC software codes used in this work, and for help and stimulating discussions during the work. O. Engler is also acknowledged for giving access to his recrystallization code and for useful input and discussions. Thanks also to NOTUR, the Norwegian Metacentre for Computational Science for providing free CPU time at their supercomputers and to the NOTUR support group at NTNU for help and guidance with the implementation and debugging of the parallel MC code.

REFERENCES

Alvi, M.H., Cheong, S.W., Suni, J.P., Weiland, H., Rollett, A.D., 2008, Cube texture in hot-rolled aluminium alloy 1050 (AA1050) - nucleation and growth behaviour, *Acta Materialia*, 56, 3098-3108.

Anderson, M.P., Grest, G.S., Srolovitz, D.J., 1989, Computer-simulation of normal grain-growth in 3 dimensions, *Phil. Mag. B*, 59, 293-329..

Brahme, A.P., 2005, *Modelling Microstructure Evolution during Recrystallization*, PhD thesis, Carnegie Mellon University, Pittsburgh, PA, USA.

Brahme, A., Alvi, M.H., Saylor, D., Friday, J., Rollett, A.D., 2006, 3D reconstruction of microstructure in a commercial purity aluminium, *Scripta Materialia*, 55, 75-80.

Brahme, A., Friday, J. Weiland, H., Rollett, A.D., 2009, Modelling texture evolution during recrystallization in aluminium, *Modelling and Simulation in Materials Science and Engineering*, 17, 015005 (20pp).

Engler, O., 1996, Nucleation and growth during recrystallization of aluminium alloys investigated by local texture analysis, *Materials Science and Technology*, 12, 859-872.

Engler, O., 1997, A simulation of recrystallization textures of alalloys with consideration of the probabilities of nucleation and growth, *Textures and Microstructures*, 28, 197-219.

Engler, O., 1999, A simulation of recrystallization textures of Al-alloys with consideration of the probabilities of nucleation and growth, *Textures and Microstructures*, 32, 197-219.

Engler, O., Löchte, L., Hirsch, J., 2007, Through-process simulation of texture and properties during the thermomechanical processing of aluminium sheets, *Acta Materialia*, 55, 5449-5463.

Fjeldberg, E., Marthinsen, K., 2010, A 3D Monte Carlo study of the effect of grain boundary anisotropy and particles on the size distribution of grains after recrystalliation and grain growth, *Computational Materials Science*, 48, 267-281.

Hassold, G.N., E.A. Holm, 1993, A fast serial algorithm for the finite temperature quenched Potts model, *Computers in Physics*, 7, 97-107.

Hassold, G.N., Holm, E.A., Miodownik, M.A., 2003, Accumulation of coincidence site lattice boundaries during grain growth, *Materials Science and Technology*, 19, 683-687.

Humphreys, F.J., Hatherly, M., 2004, Recrystallization and Related Annealing Phenomena, Elsevier, 2nd edn Oxford, Elsevier.

Liebmann, B., Lücke, K., Graham, C.D., Cahn, R.W., Dunn, C.G., 1956, Grain growth rates and orientation relationships in the recrystallization of aluminium single crystals, *Trans. Am. Inst. Metall. Engrs.*, 206, 1413-1416.

Miodownik, M.Godrey, A.W.,Holm., E.A., Hughes, D.A., 1999, On the boundary misorienation distribution functions and how to incorporate them into three-dimensional models of microstructural evolution, *Acta Mater.*, 47, 2661-2668.

Mykura, H., 1980, Grain boundary structure and kinetics, *Proc. ASM Materials Science Seminar*, ed. R.W. Baluffi, ASM Ohio, 445.

Rollett, A.D., 1997, Overview of modelling and simulation of recrystallization, *Progress in Materials Science*, 42, 79-99.

Rollett, A.D., Raabe, D., 2001, A hybrid model for mesoscopic simulation of recrystallization, *Computational Materials Science*, 21, 69-78.

Rollett, A.D., Manohar, P., 2004, The Monte Carlo Method, In: *Continuum Scale Simulation of Engineering Materials Fundamentals- Microstructures - Process Applications*, eds. Raabe, D., Roters, F., Barlat, F., and Chen L.Q. Wiley-VCH Verlag, GmbH&Co. KGaA, Weinheim, 77-114.

Sebald R., Gottstein, G., 2002, Modeling of recrystallization textures: interaction of nucleation and growth, *Acta Mater.*, 50, 1587-1598.

Vatne, H.E.,Furu, T. Ørsund, R., Nes, E., 1996, Modelling recrystallization after hot deformation of aluminium,. *Acta Mater.*, 44, 4463-4473.

NUMERYCZNA ANALIZA PROCESU ZACISKANIA TULEI

Streszczenie

W opracowaniu przedstawiono wyniki analizy numerycznej procesu zaciskania tulei między innymi na linach stalowych przy pomocy obrotowych segmentów bruzdowych. Omówiono obszary zastosowań wyrobów typu liny i cięgna oraz przedstawiono sposoby wykonywania na nich zakończeń. Analizę numeryczną procesu przeprowadzono w oparciu o metodę elementów skończonych (MES), wykorzystując komercyjny pakiet oprogramowania DEFORM - 3D. Omówiono modele geometryczne zastosowane w obliczeniach oraz wpływ kształtu wykroju na jakość wyrobu. Uzyskane wyniki analizy numerycznej wykorzystano w projekcie przyrządu do praktycznej realizacji tego procesu.

Received: February 29, 2012
Received in a revised form: May 18, 2012
Accepted: July 24, 2012